Supporting Information

Joint Electric and Magnetic Beam Deflection Experiments and Quantum Chemical Studies of MSn_{12} Clusters (M = Al, Ga, Sn): On the Interplay of Geometric Structure and Magnetic Properties in Nanoalloys

Filip Rivic,*‡ Andreas Lehr,‡ Thomas M. Fuchs, and Rolf Schäfer

Technical University of Darmstadt, Eduard-Zintl-Institut, Alarich-Weiss-Straße 8, 64287 Darmstadt, Germany.
‡ These authors contributed equally to this work.

---

1. Computational Details

1.1 Genetic Algorithm

The experimental work is complemented with a genetic algorithm-based global search of the coordination space, followed by a local structural reoptimization and frequency analyses on varying levels of theory. The global optimization was conducted by the German Improved Genetic Algorithm (GIGA)[1], which is the newest iteration of the Birmingham Cluster Genetic Algorithm (BCGA).[2–4] The calculations for MSn_{12} (M = Al, Ga, In) were performed with plane-wave density functional theory (DFT) using Quantum Espresso v6.4.1.[5,6] The PBE exchange-correlation (xc) functional[7,8] was applied within the framework of spin-restricted DFT. The ultrasoft RRKJ pseudopotentials[9,10] (10 core electrons for Al, 18 for Ga, 36 for In and 36 for Sn) with a plane-wave kinetic energy cutoff of 400 eV were employed. The box size of the unit cell is determined dynamically such that no duplicate clusters are closer than 16 Å and self-interaction can be neglected. Spin polarization was implemented and a small Methfessel-Paxton smearing[11] as well as nonlinear core corrections[12] were applied. The geometry optimizations during the GIGA iterations were performed with an electronic self-consistency criterion of 10^{-6} eV. Total energy and force convergence threshold values were set to 10^{-4} eV and 10^{-3} eV Å^{-1}, respectively.

1.2 Reoptimization and Dielectric Properties

All identified structural candidates within 4 eV relative to the lowest-energy structure were considered for local reoptimization using spin-unrestricted Gaussian orbital-based DFT with tight optimization criteria and high-density numerical grids. These calculations were carried out with Gaussian16[13] and Orca v5.0.2[14–16] employing the PBE0/def2-TZVPP[17–19] level of theory considering doublet, quartet and sextet spin configurations with the former on being the energetically most favorable throughout. Scalar relativistic corrections were effectively treated by the use of this pseudopotential-supported basis set. The choice of the xc functional/basis set combination was justified by extensive previous studies on bare tin[20–23], bare lead[24,25] and doped tin clusters.[26–29] Additionally, high symmetry configurations (I_h, T_h, O_h, D_{6h}, D_{2h}, D_{5d} and D_{3d}) built from the perfect icosahedral symmetry were reoptimized symmetry-unconstrained as well employing the xc functionals PBE0[17], B3P86[30], B3LYP[31], HSE06[32,33], LC-ωPBEh[34,35], TPSSh[36–38], M06[39] and B2PLYP[40,41] with the goal to not miss out a high-symmetry configuration. Those isomers below 0.3 eV relative to the global minimum (GM) were chosen for the calculation of electric dipole moments, unrestricted spin densities and vibrational frequencies. CCSD(T)/cc-pVTZ-PP[42,43] single-point energies on top of the PBE0/def2-TZVPP optimized geometries were computed using the domain-based local pair natural orbital (DLPNO) acceleration approach[44–47] implemented in Orca. Furthermore, the CCSD(T) energies were computed using the „NormalPNO“ criterion and extrapolated to the complete basis set limit using the two-point extrapolation for the cc-pVTZ-PP and corresponding auxiliary basis sets.[48]

1.3 Magnetic Properties

Magnetic properties comprising the g-matrix and the hyperfine coupling constant were computed with the EPR/NMR module of Orca. The scalar relativistically-parametrized second-order Douglas-Kroll-Hess (DKH2)[49] and zeroth-order regular approximation (ZORA) Hamiltonians[50] were used in combination with the accordingly recontracted basis sets DKH- and ZORA-def2-TZVPP[51] at the PBE0 level of theory. For the elements In and Sn the segmented all-electron relativistically contracted (SARC) versions together with their decontracted auxiliary basis sets (SARC/J) were implemented.[52] To efficiently speed up the calculations, the resolution of identity approximation for the Coulomb integrals and the numerical integration for the Hartree-Fock exchange (RIJCOSX)[53] was made use of with the DFT numerical interation grid precision set to „DefGrid2“. Picture-change effects were implemented throughout, for DKH up to its second-order transformation of the Hamiltonian.[49] Regarding the DKH method, the magnetic field was implemented in the free-particle Foldy-Wouthuysen transformation only for the calculation of the g-matrices.[49] All contributions to the model potentials are considered in their default settings. Furthermore, the finite-nucleus model was applied. Before invoking the EPR/NMR module it was assured that geometry optimizations for all structural isomers at the relativistic level yield insignificant differences to the nonrelativistic PBE0/def2-TZVPP results. Regarding the calculation of the g-matrices and hyperfine coupling constants, the spin-orbit coupling operators are treated by the spin-orbit mean field (SOMF) approach, specifically the RI-SOMF(1X) variant.[54] The Pople solver was used for the calculation of the coupled-pair self-consistent field (CP-SCF) equations.[50] Again to speed up the computation, the gauge origin was chosen to be the central doping atom fixed at the cartesian center (0,0,0) which was demonstated to exactly reproduce the results obtained with gauge-dependent atomic orbitals (GIAOs)[54,55] for the T_h and D_{3d} isomers. The g-matrices were calculated both at the DKH-PBE0/(SARC-)DKH-def2-TZVPP and ZORA-PBE0/(SARC-)ZORA-def2-TZVPP level of theory, yielding very similar results with differences of 0.01 in the g-value, whereas hyperfine coupling constants were only obtained using the ZORA method.

2. Cartesian Coordinates and $AlSn_{12}$ Structural Isomers

In the manuscript only structural isomers below 0.3 eV relative to the T_h GM are shown. Here, an extended list of isomers up to 1.0 eV are presented exemplary for $AlSn_{12}$ in Fig. S1. Additionally to the GA routine and the reoptimization based on high-symmetry configurations described in Sec. 1.1, structural candidates from Sn_{13} and Sn_{13}^+[23] as well as MPb_{12} and MPb_{12}^+ geometries with M=B, Al, Ga, In, Tl[56–58] were considered for reoptimization. The cartesian coordinates of all structural isomers for MSn_{12} with M=Al, Ga, In treated in this study can be found in Tab. S1.

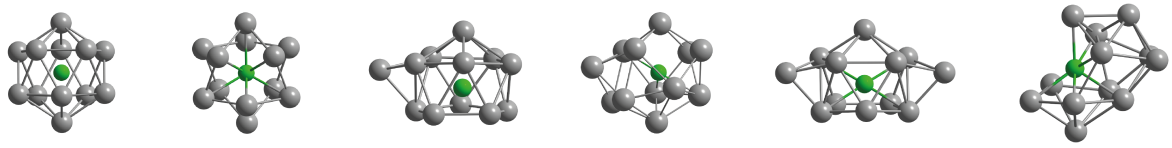

$\Delta E = 0.000$ eV	0.007 eV	0.371 eV	0.704 eV	0.775 eV	0.889 eV
T_h	D_{3d}	C_1	C_1	C_{2v}	C_1
$\mu_{el} = 0.00$ D	0.00 D	0.62 D	0.49 D	0.62 D	0.47 D

Figure S1. $AlSn_{12}$ structural isomers with an energy difference ΔE below 1 eV relative to the T_h GM at the PBE0/def2-TZVPP level of theory. The point group symmetries and electric dipole moments μ_{el} are shown.

Table S1. Summary of cartesian coordinates of all structural isomers below 0.3 eV relative to the MSn_{12} GM with M=Al, Ga, In (top and center) as well as those structural isomers below 1.0 eV relative to the $AlSn_{12}$ GM (bottom). All shown structures were reoptimized at the PBE0/def2-TZVPP level of theory.

	$AlSn_{12}$			**$GaSn_{12}$**			**$InSn_{12}$**		
	Iso1 (T_h)			Iso1 (T_h)			Iso1 (T_h)		
	x	y	z	x	y	z	x	y	z
Al/Ga/In	0.000 000	0.000 000	0.000 000	0.000 000	0.000 000	0.000 000	0.000 000	0.000 000	0.000 000
Sn	−0.371 721	−0.127 860	2.986 334	0.035 280	0.317 920	2.996 312	0.149 452	−0.483 574	3.019 058
Sn	0.371 832	0.127 658	−2.986 453	−0.035 162	−0.317 978	−2.996 235	−0.149 111	0.483 503	−3.019 129
Sn	2.853 962	−0.047 251	−0.962 796	−2.687 227	−0.617 556	−1.215 537	1.544 226	2.435 560	−1.027 143
Sn	−2.853 868	0.047 062	0.962 674	2.687 340	0.617 492	1.215 593	−1.544 051	−2.435 615	1.027 089
Sn	−2.163 160	−1.304 409	−1.641 117	1.985 424	1.686 305	−1.514 933	−0.243 406	−2.512 916	−1.731 332
Sn	2.163 284	1.304 210	1.641 005	−1.985 316	−1.686 373	1.515 002	0.243 597	2.512 895	1.731 281
Sn	1.058 402	2.608 111	−1.072 817	−0.359 700	−2.816 276	−1.009 648	−1.714 637	2.380 233	−0.875 027
Sn	−1.058 282	−2.608 310	1.072 652	0.359 815	2.816 206	1.009 741	1.714 815	−2.380 260	0.874 927
Sn	0.823 706	−2.466 539	−1.520 385	−1.179 452	2.167 361	−1.729 447	2.412 152	−0.617 891	−1.780 803
Sn	−0.823 607	2.466 384	1.520 255	1.179 565	−2.167 404	1.729 541	−2.411 953	0.617 841	1.780 842
Sn	1.840 399	−1.881 966	1.464 521	−2.340 071	1.485 092	1.182 687	2.742 165	0.463 578	1.279 568
Sn	−1.840 297	1.881 767	−1.464 707	2.340 174	−1.485 168	−1.182 597	−2.741 990	−0.463 601	−1.279 682
	$AlSn_{12}$			**$GaSn_{12}$**			**$InSn_{12}$**		
	Iso2 (D_{3d})			Iso2 (D_{3d})			Iso2 (D_{3d})		
	x	y	z	x	y	z	x	y	z
Al/Ga/In	0.000 000	0.000 000	0.000 000	0.000 000	0.000 000	0.000 000	0.000 000	0.000 000	0.000 000
Sn	0.000 000	1.913 274	2.333 081	−0.645 307	1.586 361	−2.380 307	1.340 894	1.434 346	−2.354 335
Sn	0.000 000	−1.913 274	−2.333 081	0.645 309	−1.586 364	2.380 304	−1.340 909	−1.434 354	2.354 336
Sn	0.000 000	−2.934 136	0.671 221	−0.645 343	−2.854 596	−0.183 641	−2.037 399	−2.178 534	−0.689 087
Sn	0.000 000	2.934 136	−0.671 221	0.645 344	2.854 597	0.183 638	2.037 391	2.178 531	0.689 087
Sn	−1.656 944	0.956 637	−2.333 081	0.645 297	−1.268 274	−2.563 955	0.571 196	−1.878 584	−2.354 327
Sn	1.656 944	−0.956 637	2.333 081	−0.645 294	1.268 274	2.563 954	−0.571 204	1.878 575	2.354 332
Sn	2.541 036	−1.467 068	−0.671 221	−2.567 354	−0.974 354	1.462 041	−2.905 244	0.675 060	0.689 656
Sn	−2.541 036	1.467 068	0.671 221	2.567 357	0.974 354	−1.462 043	2.905 236	−0.675 061	−0.689 655
Sn	−2.541 036	−1.467 068	−0.671 221	−2.567 405	1.753 321	0.112 815	−0.868 142	2.853 646	−0.689 089
Sn	2.541 036	1.467 068	0.671 221	2.567 409	−1.753 320	−0.112 817	0.868 134	−2.853 649	0.689 093
Sn	−1.656 944	−0.956 637	2.333 081	−2.567 347	−0.778 968	−1.574 853	−1.913 040	0.444 442	−2.353 936
Sn	1.656 944	0.956 637	−2.333 081	2.567 347	0.778 969	1.574 852	1.913 035	−0.444 445	2.353 939
				$AlSn_{12}$					
	Iso3 (C_1)			Iso4 (C_1)			Iso5 (C_{2v})		
	x	y	z	x	y	z	x	y	z
Al	0.000 000	0.000 000	0.000 000	0.000 000	0.000 000	0.000 000	0.000 000	0.000 000	0.000 000
Sn	2.364 411	1.480 973	1.298 970	−2.501 996	0.659 55	1.556 177	−0.000 454	−1.685 060	−2.443 722
Sn	4.609 656	−0.145 954	0.586 441	2.869 126	−1.001 287	−1.561 343	−2.356 695	0.095 505	1.623 048
Sn	2.184 079	−1.828 763	1.266 533	3.902 598	1.278 437	0.116 724	−0.000 469	−1.684 777	2.443 461
Sn	0.154 604	−0.215 874	3.021 980	−2.141 651	−1.920 413	−0.045 456	1.610 948	−2.652 147	−0.000 242
Sn	2.499 916	−0.140 625	−1.450 419	0.845 398	−2.875 267	−0.106 749	4.290 697	−1.385 225	−0.000 087
Sn	−0.477 322	2.513 400	1.700 213	−0.803 848	2.853 557	0.027 301	−1.507 494	2.452 416	−0.000 395
Sn	−1.177 309	−2.507 381	1.358 830	1.474 469	1.813 189	−1.620 967	2.356 235	0.095 403	−1.623 388
Sn	1.010 325	2.498 294	−1.215 724	−0.146 174	−1.269 183	2.480 707	−1.613 064	−2.653 208	−0.000 012
Sn	0.535 616	−2.526 749	−1.272 715	2.853 225	−1.137 773	1.521 496	−2.356 576	0.095 312	−1.623 330
Sn	−2.620 754	0.195 244	1.518 953	−2.568 781	0.753 638	−1.426 534	1.506 909	2.452 857	−0.000 355
Sn	−1.942 950	1.864 842	−1.021 088	1.347 857	1.678 805	1.813 982	2.356 487	0.095 736	1.622 876
Sn	−2.264 150	−1.215 126	−1.217 070	−0.122 627	−1.028 654	−2.560 907	−4.292 054	−1.383 381	−0.000 244
	$AlSn_{12}$								
	Iso6 (C_1)								
	x	y	z						
Al	0.000 000	0.000 000	0.000 000						
Sn	0.963 476	−1.269 025	−2.619 271						
Sn	0.016 634	1.629 545	−2.685 722						
Sn	2.988 724	1.247 124	−2.630 994						
Sn	2.176 115	−2.041 177	0.314 158						
Sn	−0.661 465	−2.716 274	−0.577 338						
Sn	1.477 112	2.454 705	−0.116 452						
Sn	−2.224 125	−0.539 405	−2.447 931						
Sn	3.881 558	−1.624 142	−2.103 033						
Sn	3.981 168	0.483 831	0.117 571						
Sn	−2.030 367	1.928 328	−0.423 612						
Sn	1.839 080	0.398 002	2.109 905						
Sn	−2.712 984	−0.802 196	0.485 184						

3. MO Diagrams and *g*-Factors

From the MO diagrams in Fig. 5 of the main manuscript shown for different X values, the relation between the calculated g-factors and the energy difference between the SOMO and LUMO(+1) can be further investigated. As long as the energy difference does not get too small, leading to a breakdown of the SOS expression in Eq. 4 in the manuscript, the predicted linear dependence with the inverse of the energy difference is observed computationally with a vanishingly small offset. From this, the orbital-Zeeman–spin-orbit coupling matrix elements are estimated to be of the order 1.52 eV as illustrated in Fig. S2.

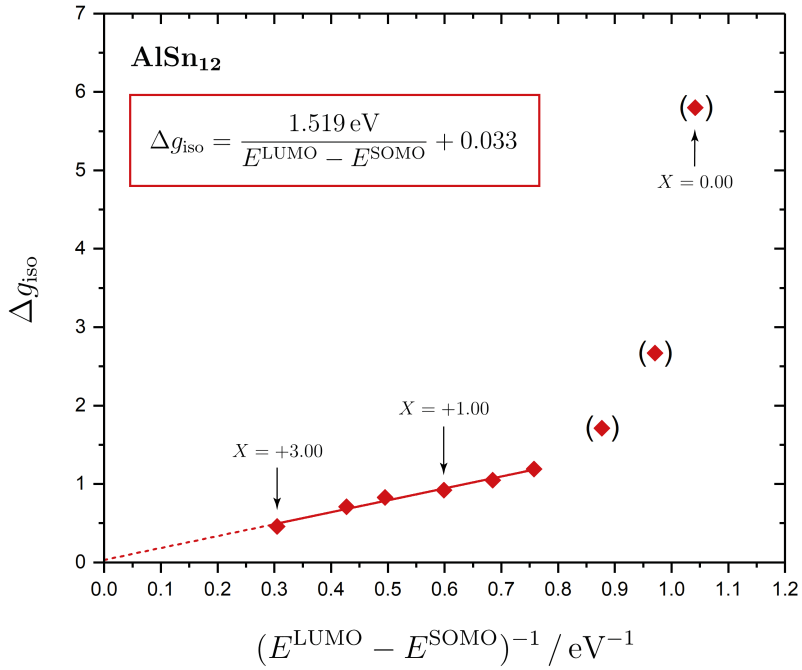

Figure S2. The Δg_{iso}-shifts computed for different X values as a function of the inverse SOMO-LUMO gap of $AlSn_{12}$ (similar to $InSn_{12}$) at the DKH-PBE0/(SARC-)DKH-def2-TZVPP level of theory. The data points for $X > 0.25$ are fitted corresponding to their linear dependence, whereas the data points in round brackets indicate the breakdown of Eq. 4 in the main manuscript. The results for $GaSn_{12}$ are conceptually comparable to the point where the energetic order of the MOs switches close to I_h symmetry ($X = 0.00$).

References

[1] M. Jäger, R. Schäfer and R. L. Johnston, *Nanoscale*, 2019, **11**, 9042–9052.

[2] R. L. Johnston, *Dalton Trans.*, 2003, **3**, 4193–4207.

[3] S. Heiles, A. J. Logsdail, R. Schäfer and R. L. Johnston, *Nanoscale*, 2012, **4**, 1109–1115.

[4] A. Shayeghi, D. Götz, J. B. Davis, R. Schäfer and R. L. Johnston, *Phys. Chem. Chem. Phys.*, 2015, **17**, 2104–2112.

[5] P. Giannozzi, S. Baroni, N. Bonini, M. Calandra, R. Car, C. Cavazzoni, D. Ceresoli, G. L. Chiarotti, M. Cococcioni, I. Dabo, A. Dal Corso, S. de Gironcoli, S. Fabris, G. Fratesi, R. Gebauer, U. Gerstmann, C. Gougoussis, A. Kokalj, M. Lazzeri, L. Martin-Samos, N. Marzari, F. Mauri, R. Mazzarello, S. Paolini, A. Pasquarello,

L. Paulatto, C. Sbraccia, S. Scandolo, G. Sclauzero, A. P. Seitsonen, A. Smogunov, P. Umari and R. M. Wentzcovitch, *J. Phys. Condens. Matter*, 2009, **21**, 395502.

[6] P. Giannozzi, O. Andreussi, T. Brumme, O. Bunau, M. Buongiorno Nardelli, M. Calandra, R. Car, C. Cavazzoni, D. Ceresoli, M. Cococcioni, N. Colonna, I. Carnimeo, A. Dal Corso, S. de Gironcoli, P. Delugas, R. A. DiStasio, A. Ferretti, A. Floris, G. Fratesi, G. Fugallo, R. Gebauer, U. Gerstmann, F. Giustino, T. Gorni, J. Jia, M. Kawamura, H.-Y. Ko, A. Kokalj, E. Küçükbenli, M. Lazzeri, M. Marsili, N. Marzari, F. Mauri, N. L. Nguyen, H.-V. Nguyen, A. Otero-de-la Roza, L. Paulatto, S. Poncé, D. Rocca, R. Sabatini, B. Santra, M. Schlipf, A. P. Seitsonen, A. Smogunov, I. Timrov, T. Thonhauser, P. Umari, N. Vast, X. Wu and S. Baroni, *J. Phys. Condens. Matter*, 2017, **29**, 465901.

[7] J. P. Perdew, K. Burke and M. Ernzerhof, *Phys. Rev. Lett.*, 1996, **77**, 3865–3868.

[8] J. P. Perdew, K. Burke and M. Ernzerhof, *Phys. Rev. Lett.*, 1997, **78**, 1396–1396.

[9] D. Vanderbilt, *Phys. Rev. B*, 1985, **32**, 8412–8415.

[10] A. M. Rappe, K. M. Rabe, E. Kaxiras and J. D. Joannopoulos, *Phys. Rev. B*, 1990, **41**, 1227–1230.

[11] M. Methfessel and A. T. Paxton, *Phys. Rev. B*, 1989, **40**, 3616–3621.

[12] S. Louie, S. Froyen and L. Cohen, *Phys. Rev. B*, 1982, **26**, 1738–1742.

[13] M. J. Frisch, G. W. Trucks, H. B. Schlegel, G. E. Scuseria, M. A. Robb, J. R. Cheeseman, G. Scalmani, V. Barone, G. A. Petersson, H. Nakatsuji, X. Li, M. Caricato, A. V. Marenich, J. Bloino, B. G. Janesko, R. Gomperts, B. Mennucci, H. P. Hratchian, J. V. Ortiz, A. F. Izmaylov, J. L. Sonnenberg, D. Williams-Young, F. Ding, F. Lipparini, F. Egidi, J. Goings, B. Peng, A. Petrone, T. Henderson, D. Ranasinghe, V. G. Zakrzewski, J. Gao, N. Rega, G. Zheng, W. Liang, M. Hada, M. Ehara, K. Toyota, R. Fukuda, J. Hasegawa, M. Ishida, T. Nakajima, Y. Honda, O. Kitao, H. Nakai, T. Vreven, K. Throssell, J. J. A. Montgomery, J. E. Peralta, F. Ogliaro, M. J. Bearpark, J. J. Heyd, E. N. Brothers, K. N. Kudin, V. N. Staroverov, T. A. Keith, R. Kobayashi, J. Normand, K. Raghavachari, A. P. Rendell, J. C. Burant, S. S. Iyengar, J. Tomasi, M. Cossi, J. M. Millam, M. Klene, C. Adamo, R. Cammi, J. W. Ochterski, R. L. Martin, K. Morokuma, O. Farkas, J. B. Foresman and D. J. Fox, *Gaussian 16, Revision C.01*, 2016.

[14] F. Neese, *Wiley Interdiscip. Rev. Comput. Mol. Sci.*, 2012, **2**, 73–78.

[15] F. Neese, *Wiley Interdiscip. Rev. Comput. Mol. Sci.*, 2018, **8**, 1–6.

[16] F. Neese, F. Wennmohs, U. Becker and C. Riplinger, *J. Chem. Phys.*, 2020, **152**, 224108.

[17] J. P. Perdew, M. Ernzerhof and K. Burke, *J. Chem. Phys.*, 1996, **105**, 9982–9985.

[18] B. Metz, H. Stoll and M. Dolg, *J. Chem. Phys.*, 2000, **113**, 2563–2569.

[19] F. Weigend and R. Ahlrichs, *Phys. Chem. Chem. Phys.*, 2005, **7**, 3297–3305.

[20] S. Schäfer, B. Assadollahzadeh, M. Mehring, P. Schwerdtfeger and R. Schäfer, *J. Phys. Chem. A*, 2008, **112**, 12312–12319.

[21] B. Assadollahzadeh, S. Schäfer and P. Schwerdtfeger, *J. Comput. Chem.*, 2010, **31**, 929–937.

[22] A. Lehr, M. Jäger, M. Gleditzsch, F. Rivic and R. Schäfer, *J. Phys. Chem. Lett.*, 2020, **11**, 7827–7831.

[23] A. Lehr, F. Rivic, M. Jäger, M. Gleditzsch and R. Schäfer, *Phys. Chem. Chem. Phys.*, 2022, **24**, 11616–11635.

[24] D. A. Götz, A. Shayeghi, R. L. Johnston, P. Schwerdtfeger and R. Schäfer, *J. Chem. Phys.*, 2014, **140**, 164313.

[25] D. A. Götz, A. Shayeghi, R. L. Johnston, P. Schwerdtfeger and R. Schäfer, *Nanoscale*, 2016, **8**, 11153–11160.

[26] S. Heiles, R. L. Johnston and R. Schäfer, *J. Phys. Chem. A*, 2012, **116**, 7756–7764.

[27] M. Gleditzsch, L. F. Pašteka, D. A. Götz, A. Shayeghi, R. L. Johnston and R. Schäfer, *Nanoscale*, 2019, **11**, 12878–12888.

[28] M. Gleditzsch, T. M. Fuchs and R. Schäfer, *J. Phys. Chem. A*, 2019, **123**, 1434–1444.

[29] M. Gleditzsch, M. Jäger, L. F. Pašteka, A. Shayeghi and R. Schäfer, *Phys. Chem. Chem. Phys.*, 2019, **21**, 24478–24488.

[30] J. P. Perdew, *Phys. Rev. B*, 1986, **33**, 8822–8824.

[31] A. D. Becke, *J. Chem. Phys.*, 1993, **98**, 5648–5656.

[32] A. V. Krukau, O. A. Vydrov, A. F. Izmaylov and G. E. Scuseria, *J. Chem. Phys.*, 2006, **125**, 224106.

[33] T. M. Henderson, A. F. Izmaylov, G. Scalmani and G. E. Scuseria, *J. Chem. Phys.*, 2009, **131**, 044108.

[34] A. F. Izmaylov, G. E. Scuseria and M. J. Frisch, *J. Chem. Phys.*, 2006, **125**, 104103.

[35] M. A. Rohrdanz, K. M. Martins and J. M. Herbert, *J. Chem. Phys.*, 2009, **130**, 054112.

[36] J. Tao, J. P. Perdew, V. N. Staroverov and G. E. Scuseria, *Phys. Rev. Lett.*, 2003, **91**, 146401.

[37] V. N. Staroverov, G. E. Scuseria, J. Tao and J. P. Perdew, *J. Chem. Phys.*, 2003, **119**, 12129–12137.

[38] V. N. Staroverov, G. E. Scuseria, J. Tao and J. P. Perdew, *J. Chem. Phys.*, 2004, **121**, 11507.

[39] Y. Zhao and D. G. Truhlar, *Theor. Chem. Acc.*, 2008, **120**, 215–241.

[40] S. Grimme, *J. Chem. Phys.*, 2006, **124**, 034108.

[41] F. Neese, T. Schwabe and S. Grimme, *J. Chem. Phys.*, 2007, **126**, 124115.

[42] D. E. Woon and T. H. Dunning, *J. Chem. Phys.*, 1993, **98**, 1358–1371.

[43] K. A. Peterson, D. Figgen, E. Goll, H. Stoll and M. Dolg, *J. Chem. Phys.*, 2003, **119**, 11113–11123.

[44] C. Riplinger, B. Sandhoefer, A. Hansen and F. Neese, *J. Chem. Phys.*, 2013, **139**, 134101.

[45] D. G. Liakos, M. Sparta, M. K. Kesharwani, J. M. Martin and F. Neese, *J. Chem. Theory Comput.*, 2015, **11**, 224108.

[46] D. G. Liakos and F. Neese, *J. Chem. Theory Comput.*, 2015, **11**, 4054–4063.

[47] C. Riplinger, P. Pinski, U. Becker, E. F. Valeev and F. Neese, *J. Chem. Phys.*, 2016, **144**, 024109.

[48] D. G. Truhlar, *Chem. Phys. Lett.*, 1998, **294**, 45–48.

[49] B. Sandhoefer and F. Neese, *J. Chem. Phys.*, 2012, **137**, 094102.

[50] F. Neese, *J. Chem. Phys.*, 2001, **115**, 11080–11096.

[51] D. A. Pantazis, X. Y. Chen, C. R. Landis and F. Neese, *J. Chem. Theory Comput.*, 2008, **4**, 908–919.

[52] J. D. Rolfes, F. Neese and D. A. Pantazis, *J. Comput. Chem.*, 2020, **41**, 1842–1849.

[53] F. Weigend, *Phys. Chem. Chem. Phys.*, 2006, **8**, 1057–1065.

[54] F. Neese, *J. Chem. Phys.*, 2005, **122**, 034107.

[55] J. Gauss, M. Kállay and F. Neese, *J. Phys. Chem. A*, 2009, **113**, 11541–11549.

[56] S. Neukermans, E. Janssens, Z. F. Chen, R. E. Silverans, P. V. Schleyer and P. Lievens, *Phys. Rev. Lett.*, 2004, **92**, 10–13.

[57] D. L. Chen, W. Q. Tian, W. C. Lu and C. C. Sun, *J. Chem. Phys.*, 2006, **124**, 154313.

[58] C. Rajesh and C. Majumder, *Chem. Phys. Lett.*, 2006, **430**, 101–107.